AMERICAN SOCIETY FOR MICROBIOLOGY | Molecular and Cellular Biology®

RESEARCH ARTICLE

Depletion of Mediator Kinase Module Subunits Represses Superenhancer-Associated Genes in Colon Cancer Cells

Emilia Kuuluvainen,[a,b]* Eva Domènech-Moreno,[a,b] Elina H. Niemelä,[a,b] Tomi P. Mäkelä[a,b]

[a]Research Program's Unit, Faculty of Medicine, University of Helsinki, Helsinki, Finland
[b]Helsinki Institute of Life Science, HiLIFE, University of Helsinki, Helsinki, Finland

ABSTRACT In cancer, oncogene activation is partly mediated by acquired superenhancers, which therefore represent potential targets for inhibition. Superenhancers are enriched for BRD4 and Mediator, and both BRD4 and the Mediator MED12 subunit are disproportionally required for expression of superenhancer-associated genes in stem cells. Here we show that depletion of Mediator kinase module subunit MED12 or MED13 together with MED13L can be used to reduce expression of cancer-acquired superenhancer genes, such as the MYC gene, in colon cancer cells, with a concomitant decrease in proliferation. Whereas depletion of MED12 or MED13/MED13L caused a disproportional decrease of superenhancer gene expression, this was not seen with depletion of the kinases cyclin-dependent kinase 9 (CDK8) and CDK19. MED12-MED13/MED13L-dependent superenhancer genes were coregulated by β-catenin, which has previously been shown to associate with MED12. Importantly, β-catenin depletion caused reduced binding of MED12 at the MYC superenhancer. The effect of MED12 or MED13/MED13L depletion on cancer-acquired superenhancer gene expression was more specific than and partially distinct from that of BRD4 depletion, with the most efficient inhibition seen with combined targeting. These results identify a requirement of MED12 and MED13/MED13L for expression of acquired superenhancer genes in colon cancer, implicating these Mediator subunits as potential therapeutic targets for colon cancer, alone or together with BRD4.

KEYWORDS BRD4, CDK19, CDK8, cancer, MED12, MED13, MED13L, Mediator, superenhancer, transcription

In cancer cells, activation of oncogenes is partly mediated by highly active enhancers termed acquired superenhancers. Thus, inhibiting cancer-acquired superenhancer-dependent transcription represents a potential way to specifically target proliferation of cancer cells. Superenhancers are enriched for many transcription regulators, including lineage-specific transcription factors Mediator and BRD4 (1–3). Superenhancer-associated genes (SE genes) have been identified to be highly sensitive to inhibition of BRD4, and targeting of BRD4 by BET (bromodomain and extraterminal motif) inhibitors has shown potential in the treatment of hematopoietic cancers (4–6). However, as with most cancer drugs, BET inhibitors also cause side effects and resistance (7, 8). Thus, there is continued interest in identifying other ways to specifically decrease expression of cancer-acquired SE genes, such as the MYC gene, alone or in combination with BET inhibitors.

The Mediator kinase module has been implicated in regulation of superenhancer-dependent transcription. The Mediator kinase module, which reversibly associates with Mediator, consists of the catalytic subunit cyclin-dependent kinase 9 (CDK8) or CDK19, its cognate cyclin (CCNC), MED12 or MED12L, and MED13 or MED13L (9). In flies, which lack the alternative subunits CDK19, MED12L, and MED13L, the functions of Cdk8 and CCNC are dependent on Med12 and Med13 (10). The kinase module regulates tran-

Received 6 November 2017 **Returned for modification** 26 November 2017 **Accepted** 27 February 2018

Accepted manuscript posted online 5 March 2018

Citation Kuuluvainen E, Domènech-Moreno E, Niemelä EH, Mäkelä TP. 2018. Depletion of Mediator kinase module subunits represses superenhancer-associated genes in colon cancer cells. Mol Cell Biol 38:e00573-17. https://doi.org/10.1128/MCB.00573-17.

Address correspondence to Emilia Kuuluvainen, emilia.kuuluvainen@helsinki.fi.

* Present address: Emilia Kuuluvainen, Institute of Biotechnology, Helsinki Institute of Life Science, HiLIFE, University of Helsinki, Helsinki, Finland.

scription through multiple mechanisms. In HeLa cells, MED12 can activate Wnt target genes through association with β-catenin (11). In mouse embryonic stem cells (mESCs), MED12 activates pluripotency genes through mediating enhancer-promoter looping via an interaction with the cohesin loading factor NIPBL (12). In mESCs, pluripotency genes are associated with superenhancers, and depletion of MED12 preferentially decreases SE gene expression in mESCs and mouse hematopoietic stem cells (mHSCs) (3, 13). This was linked to BRD4 in mouse acute myeloid leukemia (AML) cells, where MED12 depletion or BRD4 inhibition caused similar transcriptional defects, including a decrease of SE gene expression (14). In mHSCs, MED12 activates superenhancers independently of MED13, suggesting that the kinase module does not always function as an entity (13).

Colon cancer cells have also acquired superenhancers around oncogenes, including the MYC oncogene (1). Reducing MYC expression is sufficient to prevent formation of intestinal tumors of APC^{Min} mice (15). Interestingly, inhibition of BRD4 in colon cancer cells results in decreased MYC superenhancer activity and proliferation (16). Also, the Mediator kinase module has been implicated in colon cancer, as CDK8 amplification drives colon cancer cell proliferation and stimulates β-catenin activity (17). In colon cancer cells, CDK8 is also required for recruitment of BRD4 and pTEFb during elongation, suggesting an activating role in transcription for CDK8 in these cells (18, 19). Thus, we hypothesized that the Mediator kinase module subunits may be preferentially important for expression of acquired SE genes in colon cancer cells and explored whether depletion of these could be used to specifically target cancer-acquired SE genes and restrain colon cancer cell proliferation.

RESULTS

To study the potential role of the Mediator kinase module in regulating superenhancer-associated genes (SE genes) in colon cancer cells, we analyzed the transcriptome by using RNA sequencing (RNA-seq) after small interfering RNA (siRNA)-mediated depletion of several kinase module subunits and BRD4 in HCT116 colon cancer cells.

Coregulation by Mediator kinase module subunits and BRD4. Efficient depletion of all targets was noted 3 days after siRNA transfection (Fig. 1A), and RNA-seq analysis demonstrated significant changes in gene expression (Fig. 1B; see Table S1 in the supplemental material). Effects on selected highly deregulated genes were validated by quantitative PCR (qPCR) using independent siRNAs (Fig. 1C) and in a second colon cancer cell line, DLD1 (Fig. 1D). Depletion of MED12, BRD4, or MED13 together with MED13L resulted in the largest number of changed transcripts (Fig. 1B; Table S1). CDK8 depletion alone led to a small number of altered transcripts, whereas simultaneous depletion of CDK8 and CDK19 caused more changes (Fig. 1B; Table S1), as expected (14, 19). Similarly, simultaneous depletion of MED13 and MED13L led to a 10-fold increase in altered transcripts compared to the levels with separate depletions, demonstrating redundant functions (Fig. 1B; Table S1). Therefore, subsequent analyses were performed with the combined depletion of MED13 and MED13L (MED13/13L). Significant correlation was observed for siMED12- and siMED13/13L-regulated genes (Fig. 1E) (Pearson's correlation = 0.82; $P = 0.01$), including highly regulated genes, such as the ANKRD1, TNFSF18, SUSD2, and MYC genes (Table S1). MED13/13L are required for association of the kinase module with core Mediator (20), and depletion of MED13/13L caused reduced protein levels of MED12 (Fig. 1A), as shown previously (20), which may partly explain the observed correlation. However, MED12 depletion did not decrease levels of MED13/13L. Thus, the lack of significant amounts of transcripts specific to siMED13/13L (Table S1) suggests limited MED12-independent functions for MED13/13L in these cells, similar to what we showed previously for Med12-Med13 in flies (10). Significant overlap was also noted for genes regulated by depletion of CDK8/19 or MED12 and MED13/13L, including genes such as ANKRD1 and SUSD2 (Fig. 1E and F; Table S1), although the majority (around 80%) of siMED12/13/13L-regulated transcripts were unaffected by depletion of CDK8/19 (Fig. 1F). MED12 has been shown to link CDK8/19 to the kinase module via CCNC (20, 21). Accordingly, MED12 and MED13/13L

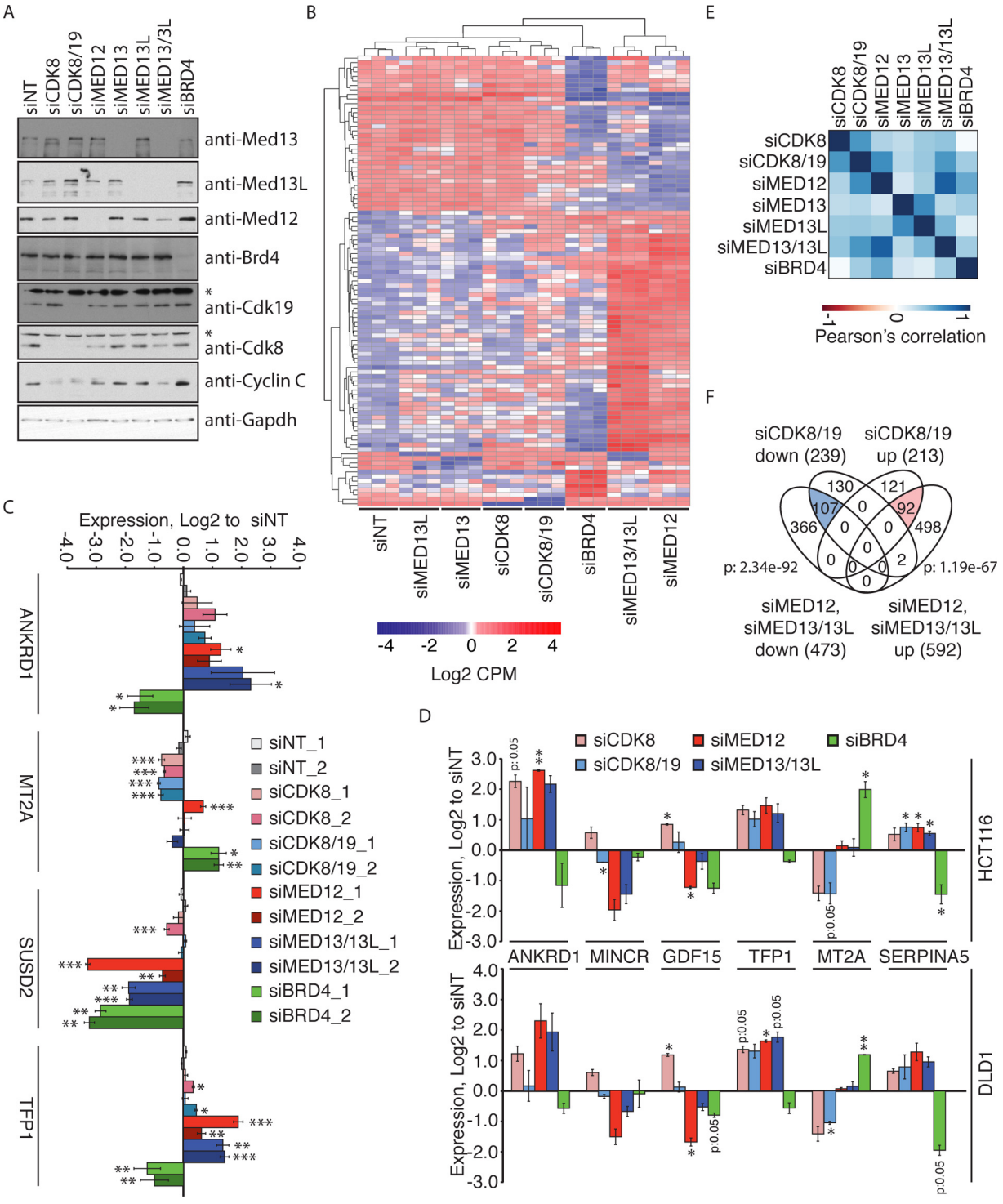

FIG 1 Transcriptome profiling of Mediator kinase module-depleted cells. (A) Western blot of HCT116 cells showing protein levels of CDK8 module subunits and BRD4 72 h after siRNA treatment. Gapdh is shown as a loading control. *, unspecific background. (B) Hierarchical clustering by Euclidean distance of 24 RNA-seq samples based on genes with ≥1.7-$\log_2$ fold expression changes relative to expression with siNT. Colors indicate $\log_2$ cpm relative to the average for all samples. Ordering of the nodes has been changed to aid in visualization, e.g., so that siNT is at the left. (C) qPCR validation of genes deregulated in RNA-seq, normalized to Gapdh expression, in HCT116 cells 72 h after treatment with the indicated siRNA (2 individual siRNAs/target). Columns and error bars show $\log_2$ fold changes relative to the average for siNT_1 and siNT_2 ± standard errors of the means (SEM) for at least 3 experiments. (D) qPCR validation of genes deregulated in RNA-seq, normalized to Gapdh expression, in HCT116 (upper panel) and DLD1 (lower panel) cells at 72 h, using pools of 4 siRNAs. Columns and error bars show $\log_2$ fold changes relative to expression with siNT ± SEM for at least 2 experiments. (E) Matrix showing Pearson's correlation coefficients between the indicated samples of genes (n = 3,840) with ≥0.59-$\log_2$ fold changes (adjusted $P < 0.05$) in any sample. (F) Venn diagram showing overlap of genes regulated in the indicated direction (≥0.59-$\log_2$ fold change; adjusted $P < 0.05$) as determined by

(Continued on next page)

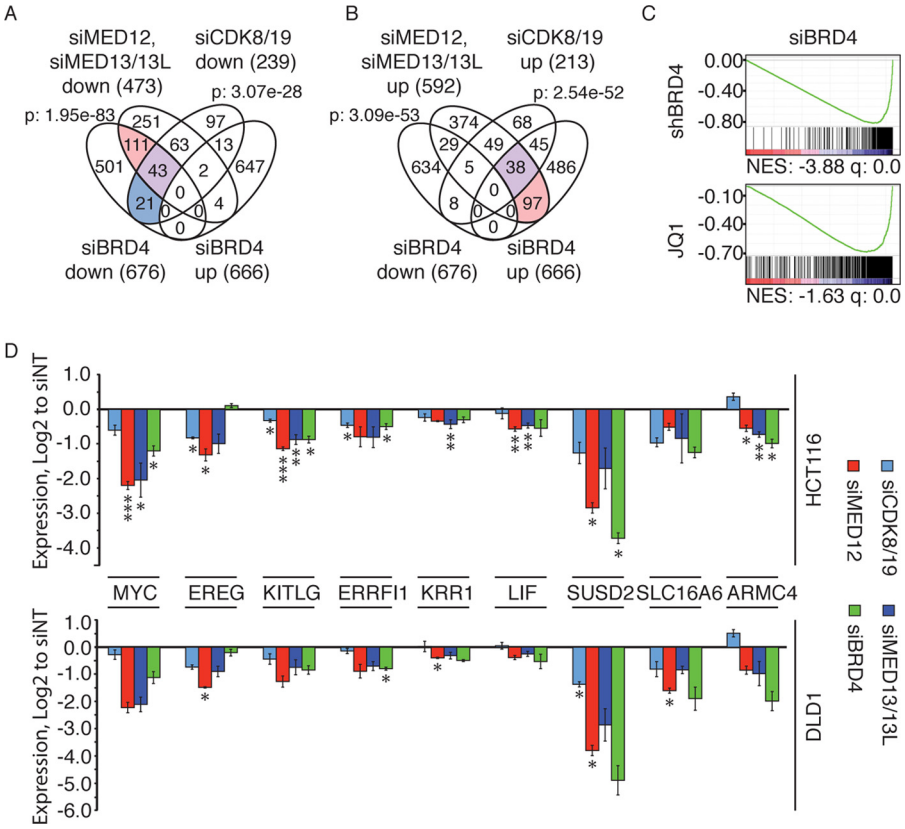

FIG 2 Coregulation by kinase module subunits and BRD4. (A and B) Venn diagrams for genes deregulated ($\geq$0.59-$\log_2$ fold change; adjusted $P < 0.05$) by the indicated siRNAs in the indicated direction as determined by RNA-seq. *P* values are for hypergeometric comparisons of genes downregulated (A) or upregulated (B) by siBRD4, siMED12, and siMED13/13L (left *P* values; red and purple areas) or by siBRD4 and siCDK8/19 (right *P* values; purple and red areas). (C) GSEA of genes downregulated by shBRD4 ($n = 362$) or JQ1 ($n = 621$) in HCT116 cells, ranked by $\log_2$ fold change in siBRD4 RNA-seq ($n = 13{,}114$). NES, normalized enrichment score. (D) Coregulation of gene expression by kinase module subunits and BRD4 was validated by qPCR. The graphs show average $\log_2$ fold changes with the indicated siRNA relative to expression with siNT for at least 2 experiments at 72 h for HCT116 (upper panel) and DLD1 (lower panel) cells. Gapdh expression was used for normalization. Error bars show SEM. *, $P < 0.05$; **, $P < 0.01$; ***, $P < 0.001$ (two-sided *t* test).

depletion resulted in reduced levels of CDK8 and CCNC, likely reflecting unstable CDK8 and CCNC proteins in the absence of MED12/13/13L-dependent association with Mediator. Interestingly, CDK8/19 depletion caused a slight increase of MED13/13L proteins (Fig. 1A), similar to the previously observed result of CDK8/19 inhibition by cortistatin A (22). This increase of MED13/13L in siCDK8/19 samples might partly explain the lower magnitude of regulation observed for many genes regulated by both CDK8/19 and MED12/13/13L depletion, such as the MYC or SUSD2 genes (Table S1).

We next investigated potential coregulation of kinase module subunits and BRD4 in these cells and observed significant overlap in regulated transcripts altered by depletion of BRD4 and both MED12 and MED13/13L. Coregulation was also observed between BRD4 and CDK8/19 (e.g., for SUSD2, MYC, TNFSF18, and HS3ST1) (Fig. 2A and B; Table S1). A previous study using the CDK8/19 inhibitor cortistatin A in AML cells did not note this coregulation (23). Transcripts regulated by siRNA-mediated depletion of BRD4 corresponded to those identified in a previous analysis using short hairpin RNA

FIG 1 Legend (Continued)
RNA-seq with siCDK8/19 or siMED12 and siMED13/13L samples. Indicated *P* values are for hypergeometric comparisons of siCDK8/19- to siMED12- and siMED13/13L-downregulated (left; blue area) and -upregulated (right; red area) genes. *, $P < 0.05$; **, $P < 0.01$; ***, $P < 0.001$ (two-sided *t* test).

(shRNA)-mediated knockdown of BRD4 or the BET inhibitor JQ1 (Fig. 2C). Coregulation by the Mediator kinase module and BRD4 was confirmed by qPCR for both HCT116 and DLD1 cells (Fig. 2D). Taken together, our results indicate transcriptional coregulation by the Mediator kinase module and BRD4 in colon cancer cells.

MED12 and MED13/MED13L are disproportionally required for expression of cancer-acquired superenhancer-associated genes. Several genes previously identified to associate with superenhancers in colon cancer cells (286 SE genes) (1) showed decreased expression following depletion of Mediator kinase module subunits or BRD4 (Table S2). This was validated for the MYC, EREG, KITLG, ERRFI1, KRR1, LIF, SUSD2, SLC16A6, and ARMC4 genes in HCT116 and DLD1 cells (Fig. 2D). Although SE genes were coregulated by depletion of kinase module subunits and BRD4, e.g., the MYC and EREG genes were more clearly affected by MED12/13/13L depletion, whereas BRD4 depletion had the strongest effect on SUSD2 gene expression (Fig. 2D). To examine if the Mediator kinase module subunits and BRD4 are disproportionally required for SE gene expression, we compared expression changes in the SE gene set ($n = 286$) to expression changes of other expressed genes (non-SE genes) in the different RNA-seq samples. SE genes, on average, were suppressed following depletion of CDK8/CDK19, MED12, MED13/13L, and BRD4 (Fig. 3A), whereas non-SE genes showed comparable levels of up- and downregulation. Accordingly, genes downregulated >1.5-fold ($P < 0.05$) by CDK8/19, MED12 and MED13/13L, or BRD4 depletion showed significant overlap with SE genes, with the most striking overlap seen for siMED12/13/13L-regulated genes (Fig. 3B). Importantly, no significant overlap was seen between SE genes and genes upregulated >1.5-fold by CDK8/19, MED12 and MED13/13L, or BRD4 depletion (Fig. 3C), demonstrating preferential downregulation of SE genes by depletion of kinase module subunits and BRD4. To investigate whether the preference of the Mediator kinase module and BRD4 for SE genes is also reflected in the level of downregulation, we compared fold changes of SE and non-SE genes that showed significant ($P < 0.05$) downregulation by the different siRNA treatments (Fig. 3D). Interestingly, MED12 and MED13/13L depletion disproportionally decreased SE genes compared to other downregulated genes, whereas no significant difference was noted with CDK8/19 and BRD4 depletion.

As cancer cells contain acquired superenhancers not present in normal cells, we investigated the impact of MED12, MED13/13L, and BRD4 depletion on 158 genes associated with superenhancers specifically in colon cancer cells but not in normal colon cells (cancer SE genes) (Table S2) (1). Interestingly, cancer SE genes were preferentially associated with decreased expression following depletion of MED12, MED13/13L, or BRD4 in gene set enrichment analyses (GSEA) (Fig. 3E) and hypergeometric comparisons (Fig. 3F). This was not noted with a control set of a randomly selected comparable number ($n = 158$) of SE genes specific for normal colon cells (Fig. 3E and F). Among the cancer SE genes with the strongest downregulation in MED12- and MED13/13L-depleted cells were the SUSD2, MYC, HS3ST1, CYP24A1, EREG, and KITLG genes (Fig. 3G). Preference for cancer SE genes was less evident for BRD4 (Fig. 3E and F, compare cancer SE and colon SE data, and Fig. 3G). Taken together, the results demonstrate a disproportional requirement of MED12 and MED13/13L for cancer SE gene expression and suggest that, for colon cancer cells, a decrease of cancer SE genes is better achieved with MED12 or MED13/13L depletion than with BRD4 depletion.

Depletion of MED12, MED13/13L, and BRD4 leads to decreased H3K27 acetylation on cancer superenhancers. Superenhancers are association with highly expressed genes and characterized by high levels of histone H3 K27 acetylation (H3K27ac) (3). To investigate if MED12/13/13L and BRD4 are specifically required for high-activity SE genes, we first compared expression levels of siMED12/13/13L- and siBRD4-regulated SE genes. Both MED12/13/13L- and BRD4-dependent and -independent SE genes were highly expressed in control (siNT) samples (Fig. 4A). Interestingly, H3K27ac levels were higher on superenhancers associated with MED12/13/13L- or BRD4-dependent genes than on superenhancers associated with genes not dependent on MED12/13/13L or BRD4 (Fig. 4B). Importantly, MED12 depletion resulted in decreased

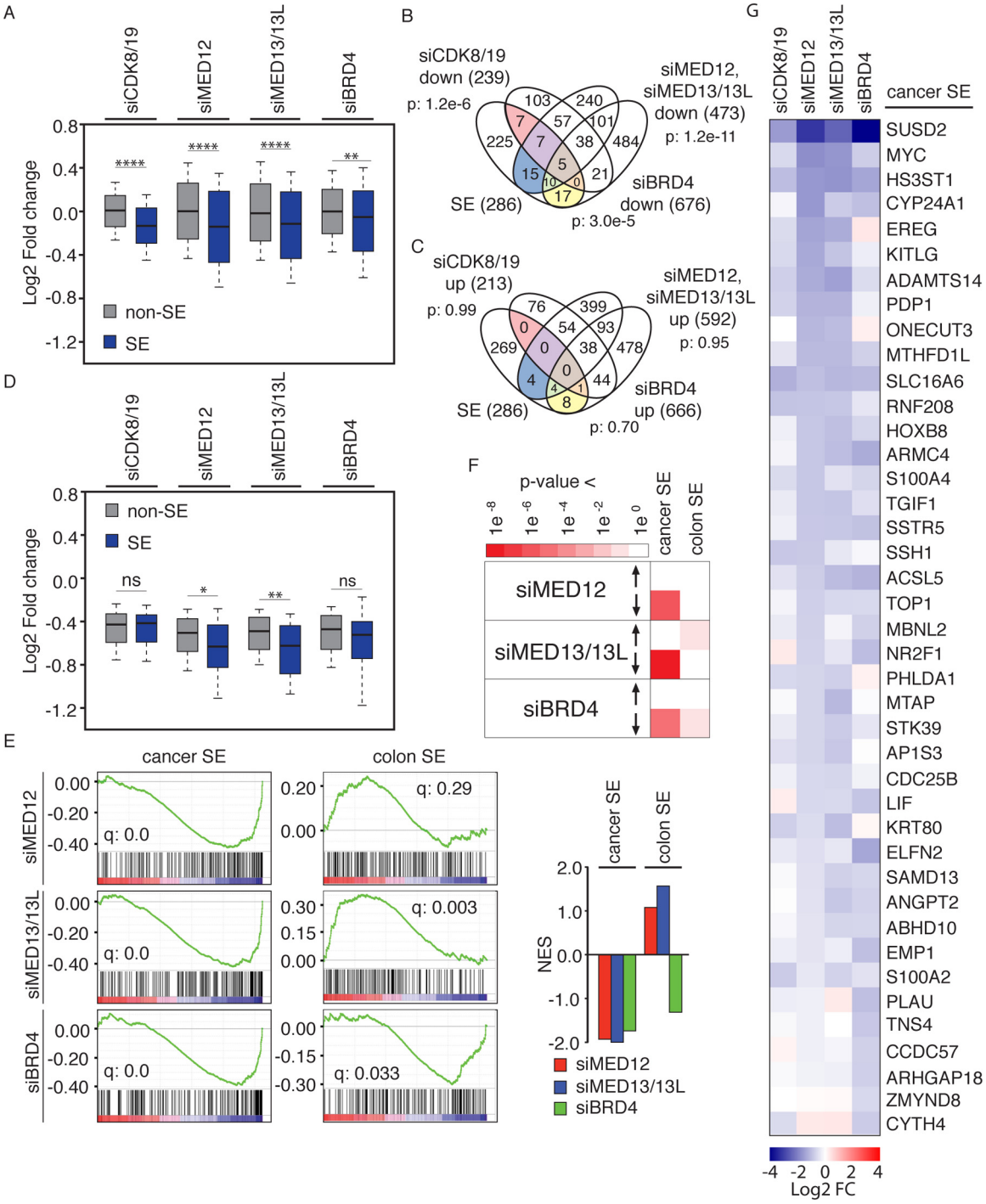

FIG 3 Disproportional requirement of MED12/13/13L for cancer-acquired SE gene expression. (A) Log_2 fold changes relative to expression with siNT for all expressed non-SE (gray; n = 12,829) and SE (blue; n = 286) genes in the indicated samples for RNA-seq. (B and C) Venn diagrams showing overlap of SE genes with genes downregulated (B) or upregulated (C) ≥0.59 log_2 fold (adjusted $P < 0.05$) in RNA-seq analysis of siCDK8/19, siMED12 and siMED13/13L, or siBRD4 samples. Indicated P values are for hypergeometric comparisons of siCDK8/19-regulated genes to SE genes (left; red, purple, brown, and orange areas), siMED12- and siMED13/13L-regulated genes to SE genes (right; purple, brown, blue, and green areas), and siBRD4-regulated genes to SE genes (bottom; brown, orange, green, and yellow areas). (D) Log_2 fold changes relative to expression with siNT for decreased (adjusted $P < 0.05$) non-SE (gray) and SE (blue) genes in the indicated samples by RNA-seq (n = 864/66 for non-SE/SE genes and siCDK8/19, 2,427/98 for siMED12, 2,614/89 for siMED13/13L, and 1,945/75 for siBRD4). (E) GSEA of all genes associated with a superenhancer specifically in colon cancer cells but not in colon cells (cancer SE; n = 158) or of an equally sized control set of genes associated with a superenhancer in colon but not colon cancer cells (colon SE; n = 158), ranked by log_2 fold change in siMED12, siMED13/13L, or siBRD4 RNA-seq compared to the result for siNT RNA-seq (n = 13,114). Columns at the right show normalized enrichment scores (NES) for the indicated comparisons. (F) Matrix showing P values for hypergeometric comparisons of cancer SE (n = 158) or colon SE (n = 158) genes and genes upregulated (rows 1, 3, and 5; n = 1,015, 1,068 and 666 genes, respectively) or downregulated (rows 2, 4, and 6; n = 956, 930, and 676 genes, respectively) ≥0.59 log_2 fold (adjusted

(Continued on next page)

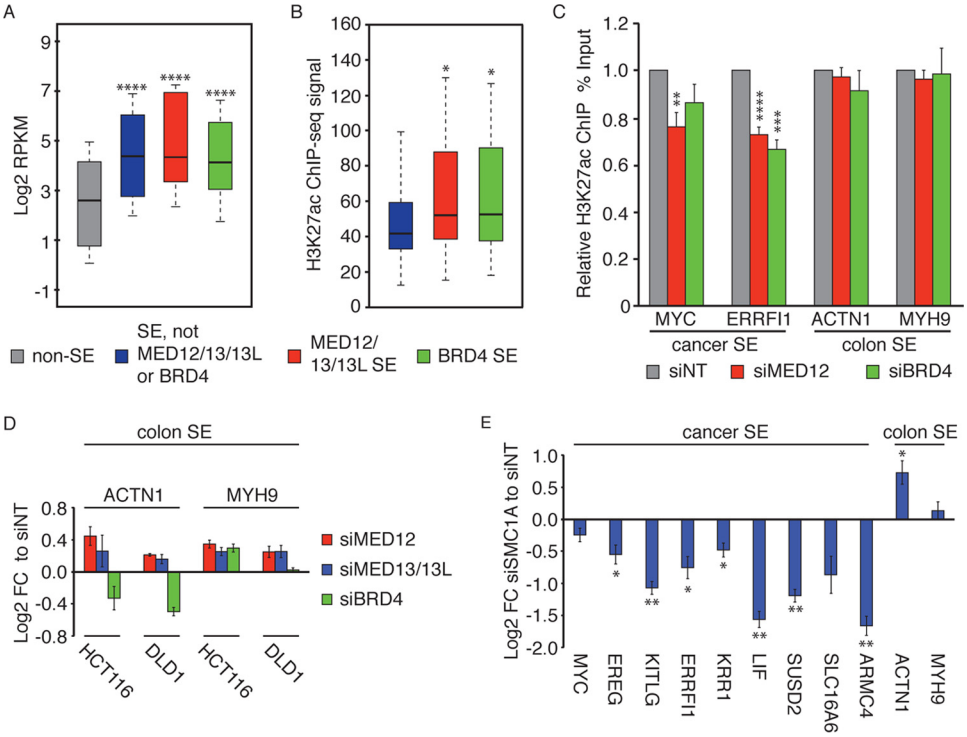

FIG 4 Decreased H3K27 acetylation on cancer superenhancers by MED12 or MED13/13L depletion. (A) Expression (mean $\log_2$ reads per kilobase per million [RPKM]) in siNT samples of non-SE genes (gray; $n = 12{,}829$), non-MED12/13/13L- or -BRD4-regulated SE genes ($n = 149$), or SE genes downregulated (adjusted $P < 0.05$) by siMED12 and siMED13/13L (red; $n = 75$) or siBRD4 (green; $n = 75$). (B) H3K27ac ChIP-seq signals (reads per million per kilobase pair [RPM/kbp]) at superenhancers associated with genes not affected by siMED12, siMED13/13L, or siBRD4 (blue; $n = 149$) or downregulated (adjusted $P < 0.05$) by siMED12 and siMED13/13L (red; $n = 75$) or siBRD4 (green; $n = 75$). Box-and-whisker plots in panels A and B show medians and first and third quartiles with standard deviations (SD) for $\log_2$ RPKM (A) and RPM/kbp (B). (C) H3K27ac levels at cancer SE and colon SE enhancers, determined by ChIP-qPCR analysis of HCT116 cells 72 h after siRNA treatment. Relative percentages of input compared to the signal for siNT treatment are shown as averages ± SEM for 4 independent ChIP samples, using primers against 2 different sites at the enhancer. (D) Expression by qPCR of control colon SE genes in HCT116 or DLD1 cells following treatment with the indicated siRNA. The data show average $\log_2$ fold changes at 72 h relative to expression with siNT for 2 experiments. Gapdh expression was used for normalization. Error bars show SEM. The changes are not significant, except that for ACTN1 in the siMED12 sample in DLD1 cells ($P = 0.049$). (E) Expression by qPCR of cancer SE genes and control colon SE genes in HCT116 cells following depletion of SMC1A. The data show average $\log_2$ fold changes at 72 h relative to expression with siNT for 4 samples. Gapdh expression was used for normalization. Error bars show SEM. *, $P < 0.05$; **, $P < 0.01$; ***, $P < 0.001$ (two-sided t test).

H3K27ac levels on the cancer-acquired superenhancers associated with the MYC and ERRFI1 genes (Fig. 4C). As a control, we analyzed H3K27ac levels on enhancers of genes which are associated with a superenhancer (based on high H3K27ac levels) only in normal colon cells, such as ACTN1 and MYH9 (1). MED12 depletion in colon cancer cells did not affect H3K27ac levels on enhancers of ACTN1 and MYH9 (Fig. 4C). Similarly, MED12 or MED13/13L depletion did not decrease the expression of these genes (Fig. 4D). A similar trend was noted following depletion of BRD4 (Fig. 4C and D). In mESCs, depletion of MED12 or the cohesin subunit SMC1A, important for mediating looping of enhancers to promoters, leads to a decrease of superenhancer-associated pluripotency gene expression (12). In our study, depletion of SMC1A caused effects similar to those of MED12/13/13L depletion, with decreased expression of cancer-acquired SE genes

FIG 3 Legend (Continued)
$P < 0.05$) by the indicated siRNA. (G) Heat map of cancer SE genes downregulated ≥0.59 $\log_2$ fold (adjusted $P < 0.05$) by siCDK8/19, siMED12, siMED13/13L, or siBRD4. Colors indicate $\log_2$ fold changes relative to the average for siNT samples. Genes are sorted by $\log_2$ fold change in the siMED12 sample. Box-and-whisker plots in panels A and D show medians and first and third quartiles of $\log_2$ fold changes with standard deviations (SD) for the indicated samples. *, $P < 0.01$; **, $P < 0.001$; ***, $P < 0.0001$; ****, $P < 0.00001$; ns, nonsignificant (two-sided t test).

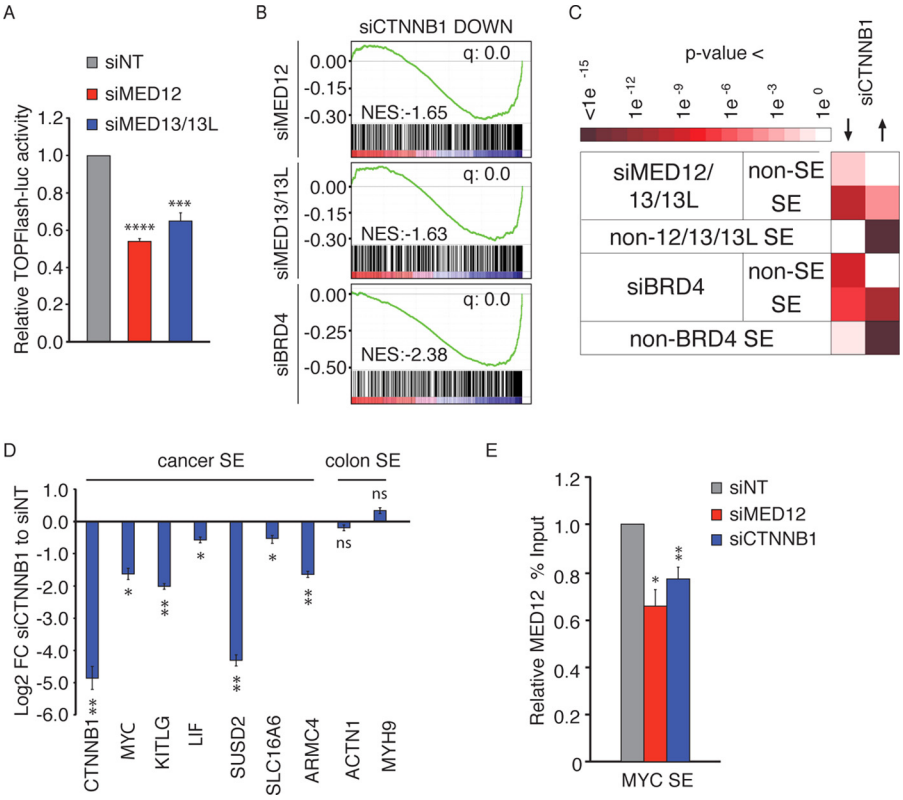

FIG 5 β-Catenin dependency of MED12- and MED13/MED13L-regulated SE genes. (A) TOPFlash-luciferase activity normalized to TK-renilla-luciferase activity in Caco-2 colon cancer cells 72 h following depletion of MED12 or MED13/13L compared to the activity with siNT. Columns show averages and SEM for 6 samples. (B) GSEA of genes downregulated by siCTNNB1 in HCT116 cells, ranked by expression in siMED12, siMED13/13L, or siBRD4 RNA-seq. NES, normalized enrichment score. (C) Matrix showing *P* values for hypergeometric comparisons of non-SE genes (rows 1 and 4; $n = 1{,}552$ and 1,945, respectively), SE genes downregulated (adjusted $P < 0.05$) by siMED12 and siMED13/13L or siBRD4 (rows 2 and 5; $n = 75$ and 75, respectively), or SE genes unaffected by siMED12 and siMED13/13L (non-12/13/13L SE) or siBRD4 (non-BRD4 SE) (rows 3 and 6; $n = 211$ and 211, respectively) to genes downregulated (left column; $n = 448$) or upregulated (right column; $n = 632$) by depletion of CTNNB1 in HCT116 cells. (D) Expression by qPCR of cancer SE genes and control colon SE genes in HCT116 cells following depletion of CTNNB1. Data show average $\log_2$ fold changes at 72 h relative to the expression with siNT for 3 samples. Gapdh expression was used for normalization. Error bars show SEM. (E) MED12 level at the MYC cancer superenhancer, determined by ChIP-qPCR analysis of HCT116 cells 72 h after treatment with the indicated siRNA. Relative percentages of input compared to the value for siNT are shown as averages and SEM for 4 (siCTNNB1) or 2 (siMED12) independent ChIP samples, using primers against 2 different sites at the enhancer. *, $P < 0.05$; **, $P < 0.01$ (two-sided *t* test).

but not control colon SE genes (Fig. 4E). To summarize, depletion of MED12/13/13L and BRD4 resulted in decreased activity, as measured by H3K27ac levels, of superenhancers associated with genes coregulated by MED12/13/13L, BRD4, and cohesin in colon cancer cells.

MED12- and MED13/MED13L-regulated superenhancer-associated genes are dependent on β-catenin. The requirement of MED12/13/13L for expression of highly expressed SE genes suggested the possible involvement of some highly active signaling pathway, such as Wnt signaling. Colon cancer superenhancers are sensitive to Wnt pathway activity (24), and MED12 has been linked to Wnt signaling activation in HeLa cells through an association with β-catenin (11). Depletion of MED12 or MED13/13L significantly reduced Wnt signaling reporter activity, suggesting that MED12 and MED13/13L are also required for Wnt pathway activation in colon cancer cells (Fig. 5A). We therefore asked if Wnt pathway activity underlies the selectivity of MED12/13/13L toward SE genes, such as MYC. For this purpose, we compared the RNA-seq profiles following depletion of MED12, MED13/13L, and BRD4 to the RNA-seq profile of HCT116 cells after siRNA-mediated depletion of β-catenin (25). Genes downregulated by MED12/

13/13L depletion showed only modest enrichment for β-catenin-dependent genes in this comparison (for non-SE genes, $n = 1,551$) (Fig. 5B and C). Interestingly, whereas only 4.6% (72/1,551 genes) of MED12/13/13L-dependent non-SE genes were significantly downregulated by β-catenin depletion, 22.6% (17/75 genes) of the MED12/13/13L-dependent SE genes were β-catenin dependent (Fig. 5B). In contrast, coregulation by BRD4 and β-catenin (Fig. 5B) was more evident for BRD4-dependent non-SE genes than for BRD4-dependent SE genes (Fig. 5C). Importantly, SE genes that were not dependent on MED12/13/13L showed enrichment for β-catenin-repressed genes (56/211 genes), whereas only 5.2% were decreased by β-catenin depletion (Fig. 5B). Again, this difference was more evident for comparing MED12/13/13L-regulated SE genes to non-MED12/13/13L-regulated SE genes than for comparing BRD4-regulated SE genes to non-BRD4-regulated SE genes (Fig. 5B). Taken together, these data suggest that β-catenin dependency is a determinant for MED12/13/13L-regulated SE genes. We confirmed that cancer SE genes (the MYC, KITLG, LIF, SUSD2, SLC16A6, and ARMC4 genes) were also β-catenin dependent in our HCT116 cells (Fig. 5D). As Wnt activation in nonmalignant cells has been shown to involve association with the Mediator MED12 subunit (11), we next investigated the effect of β-catenin depletion on chromatin-bound MED12. MED12 depletion resulted in reduced binding of MED12 at the MYC superenhancer, demonstrating specificity of the antibody. Importantly, depletion of β-catenin resulted in a comparable reduction of MED12 on the MYC superenhancer, suggesting that β-catenin regulates MYC in colon cancer cells partly via superenhancer-bound MED12 (Fig. 5E).

Decreased MYC levels and proliferation following MED12 and MED13/MED13L depletion. Consistent with the observed decrease of MYC expression following depletion of MED12 and MED13/13L (Fig. 2D), MYC target genes were identified by GSEA with 50 hallmark gene set as the most significantly enriched signature of genes downregulated in MED12- and MED13/13L-depleted cells (Fig. 6A; Table S3). As MYC itself was strongly downregulated at the mRNA level, MYC target genes are likely to represent a secondary effect of MYC downregulation. As expected, the reduced mRNA levels were reflected as a strong reduction of MYC protein levels following MED12 and MED13/13L depletion in HCT116 cells (Fig. 6B), whereas BRD4 depletion had more limited effects on MYC and its target genes (Fig. 6A and B). Interestingly, the strong effect of MED12 and MED13/13L on MYC was not noted in nonmalignant control colon cells (Fig. 6B and C) that expressed low levels of the MYC gene and other cancer SE genes (Fig. 6D). MED12 and MED13/13L depletion also led to decreases in cell numbers at 3 days, specifically in colon cancer cells, and did not affect the number of control colon cells (Fig. 6E). In agreement with this, MED12 depletion also affects proliferation of AML blasts but not that of control MEF cells (14). The reduction in cell number was associated with a decrease in cells in S phase at 72 h as measured by 5-ethynyl-2′-deoxyuridine (EdU) incorporation (Fig. 6F), indicating that MED12/13/13L are required for colon cancer cell proliferation. Importantly, MED12 or MED13/13L depletion did not affect proliferation at 48 h (Fig. 6F and G), whereas downregulation of MYC, as well as that of other SE genes, was noted already 24 h after MED12/13/13L depletion (Fig. 6H). Thus, these results are consistent with the notion that the proliferation defect following MED12/13/13L depletion is mediated at least partly by decreased expression of MYC, which is critical for colon cancer progression (26).

Dual targeting of BRD4 together with MED12 or MED13/MED13L causes a strong decrease of superenhancer-associated gene expression and has additive effects on proliferation. As SE genes showed partly differential regulation by MED12/13/13L and BRD4 (Fig. 2D, 3B, 5B, and 6H), we hypothesized that SE gene expression is dependent on MED12/13/13L and BRD4 partly due to distinct mechanisms. To investigate this, we analyzed the effects of combining BRD4 depletion with MED12 or MED13/13L depletion on cancer SE genes (Fig. 7A). Some genes, such as the MYC and EREG genes, were downregulated more strongly by MED12/13/13L depletion than by BRD4 depletion. In contrast, others, such as the SUSD2 and SLC16A6 genes, were downregulated more strongly by BRD4 depletion than by MED12 or MED13/13L

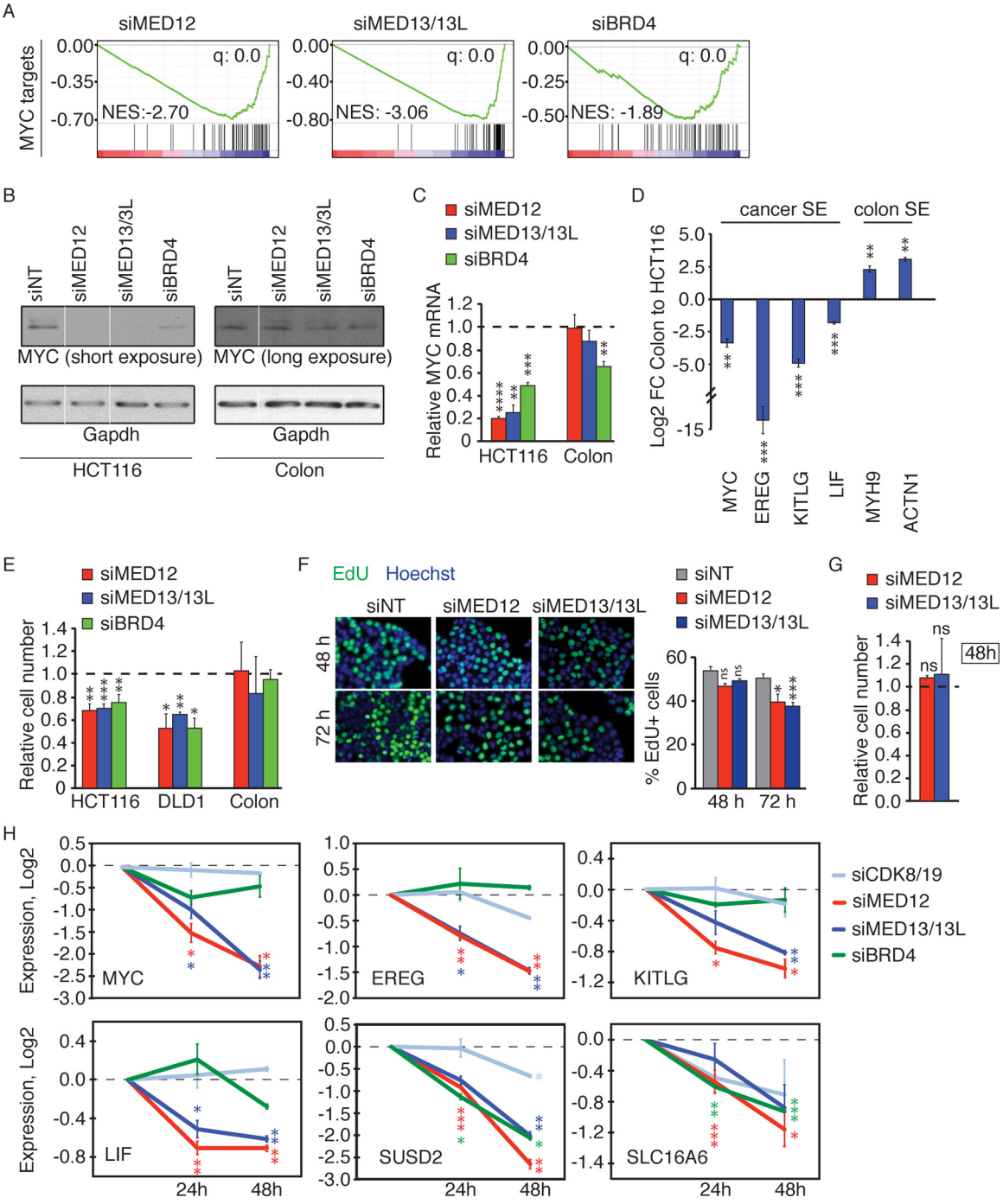

FIG 6 Decreased MYC expression and proliferation after MED12 or MED13/13L depletion in colon cancer cells. (A) GSEA of MYC target (V2) hallmark gene set against genes (n = 13,114), ranked by $\log_2$ fold change in siMED12, siMED13/13L, or siBRD4 RNA-seq compared to the results of siNT RNA-seq. NES, normalized enrichment score. (B) Western blotting with anti-MYC and anti-Gapdh antibodies 72 h after treatment of HCT116 and colon CCD841 CoN cells with the indicated siRNA. Removed lanes are indicated with vertical lines. Note the exposure difference between HCT116 and CCD841 CoN cells. (C) Relative MYC mRNA expression normalized to Gapdh expression. Data are fold changes (qPCR) in expression relative to expression in the same cells treated with siNT for HCT116 and colon CCD841 CoN cells 72 h after treatment with the indicated siRNA and are averages for 4 experiments. Error bars show SEM. The data for HCT116 cells include data from Fig. 2D. (D) Expression ($\log_2$ fold change) of cancer SE and colon SE genes in colon CCD841 CoN cells compared to that in colon cancer HCT116 cells. Data are averages and SEM for 4 samples. (E) Number of cells relative to that in the siNT sample at 72 h. Data are averages for 9 experiments (HCT116 cells; except for BRD4 [8 experiments]), 3 experiments (DLD1 cells), and 6 experiments (CCD841 CoN cells). (F) Representative images and quantification of EdU-positive cells 48 and 72 h after treatment with the indicated siRNA for at least 4 experiments. An average of 10 images were quantified for each experiment. Error bars show SEM. (G) Number of HCT116 cells relative to that in the siNT sample at 48 h. Data are averages for 3 experiments, and error bars show SEM. (H) Expression (mean $\log_2$ fold change in qPCR ± SEM) compared to that with siNT in 2 (siCDK8/19 and siBRD4) and 3 (siMED12 and siMED13/13L) experiments for cancer SE genes, normalized to Gapdh expression, 24 and 48 h after treatment of HCT116 cells with the indicated siRNA. *, $P < 0.05$; **, $P < 0.01$; ***, $P < 0.001$ (two-sided t test).

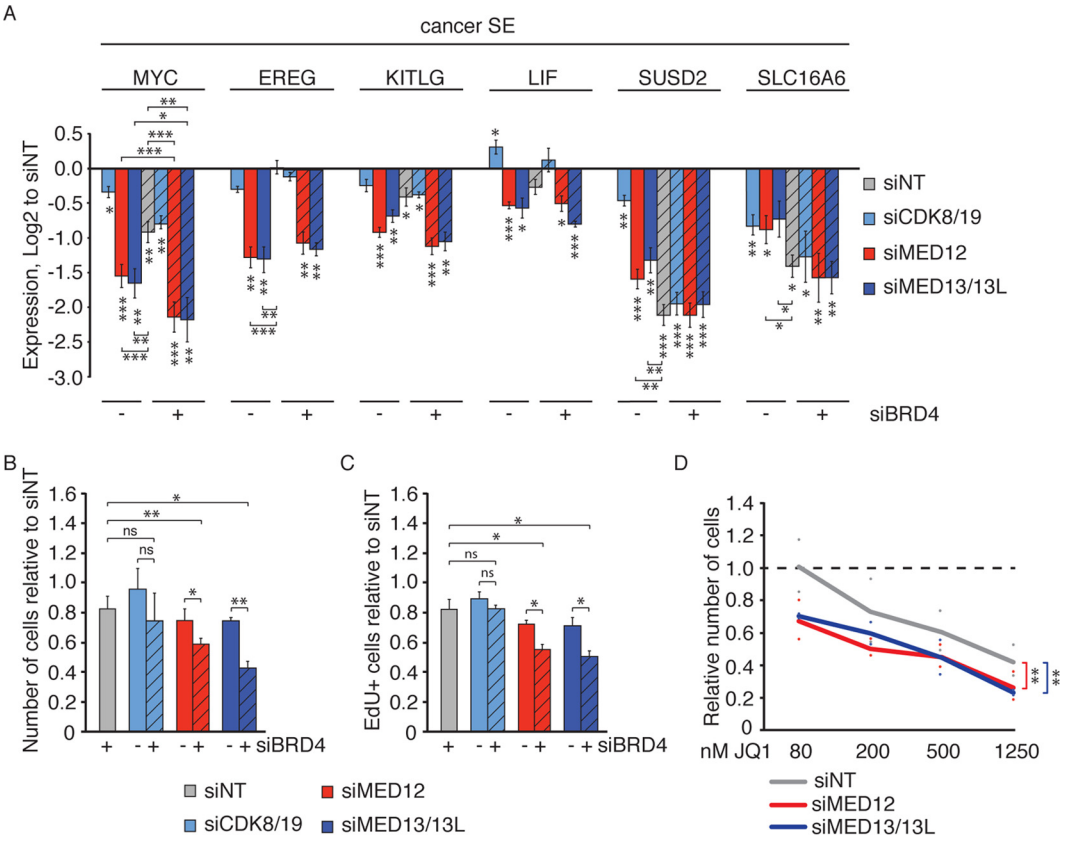

FIG 7 Stronger effects on SE gene expression and colon cancer cell proliferation by dual targeting of MED12 or MED13/13L with BRD4. (A) Expression of cancer SE genes normalized to Gapdh expression 48 h after treatment of HCT116 cells with the indicated siRNA, shown as mean $\log_2$ fold changes by qPCR compared to expression with siNT ± SEM for 5 experiments. (B) Number of cells at 72 h relative to that of the siNT sample. Data are averages and SEM for 5 experiments with the indicated siRNA. (C) Number of EdU-positive cells relative to that with siNT. Data are averages and SEM for 2 experiments with 2 replicates each 72 h after treatment with the indicated siRNA. An average of 10 images were quantified for each replicate. (D) Number of HCT116 cells relative to that in the siNT-treated sample (mean ± SEM for 3 experiments) 72 h after treatment with the indicated siRNA. Cells were treated with the indicated concentrations of JQ1 for the last 24 h. *, $P < 0.05$; **, $P < 0.01$; ***, $P < 0.001$ (two-sided *t* test).

depletion (Fig. 7A). Importantly, combined depletion of MED12 or MED13/13L and BRD4 resulted in strong decreases of all cancer SE genes (Fig. 7A). Interestingly, combined depletion of MED12 or MED13/13L and BRD4 resulted in additive effects on MYC expression, suggesting partly independent mechanisms for MYC regulation by MED12/13/13L and BRD4. Accordingly, combining BRD4 depletion with depletion of MED12 or MED13/13L caused additive effects on cell proliferation (Fig. 7B and C). In contrast, combined depletion of BRD4 with that of CDK8 and CDK19 did not increase the effect on proliferation or SE gene expression (Fig. 7A to C). The limited effect of CDK8/19 depletion on SE gene expression observed here is in line with a recent study that found CDK8 deletion to be insufficient to reduce the intestinal tumor burden of APC^{Min} mice (27). Furthermore, a significant increase in the growth-inhibitory effect was observed by combining inhibition of BRD4 by JQ1 (28) with MED12 or MED13/13L depletion (Fig. 7D), implicating dual targeting of these Mediator kinase module subunits and BRD4 as a potential therapeutic opportunity in the future.

DISCUSSION

Our study on the role of Mediator kinase module subunits as regulators of SE gene expression in colon cancer cells revealed an interesting susceptibility of cancer-acquired SE genes to regulation by MED12 and MED13/13L. The RNA-seq analysis demonstrated significant redundancy between MED13 and MED13L, where single depletions had modest effects on mRNA levels but the combined depletion resulted in 10-fold more

deregulated transcripts. The observed similarity of siMED12 and siMED13/13L RNA-seq results suggests that the majority of MED13/13L functions are mediated via MED12 in human cells. In contrast, limited overlap was noted for transcripts regulated by depletion of MED12/13/13L and those regulated by depletion of CDK8/19, in line with what we previously showed for Med12, Med13, and Cdk8 in flies (10).

Importantly, MED12 and MED13/13L were found to be disproportionally required for expression of cancer-acquired SE genes. Many of the MED12/13/13L-dependent SE genes, including MYC, were also dependent on β-catenin, possibly reflecting an interaction of MED12 and β-catenin (11) on superenhancers with abundant TCF4 sites (24). Importantly, MED12/13/13L-independent SE genes were not decreased by β-catenin depletion, suggesting that β-catenin dependency is a determinant for MED12/13/13L-regulated SE genes. The observed correlation of non-MED12/13/13L/BRD4-regulated SE genes with genes derepressed by β-catenin depletion will be an interesting area for further studies. Importantly, β-catenin depletion resulted in decreased MED12 levels on the MYC superenhancer, suggesting β-catenin-dependent recruitment of MED12 as a possible mechanism for MED12/13/13L-dependent activation of colon cancer SE genes. MED12 depletion resulted in decreased H2K27ac specifically on superenhancers, and expression of MED12/13/13L-dependent cancer SE genes was also dependent on cohesin. Both cohesin and the histone acetyltransferase p300 have previously been associated with MED12 (12, 13) and are disproportionally enriched on superenhancers in mESCs (1). It is thus likely that p300 and cohesin are involved in mediating the disproportionate requirement of MED12/13/13L for highly expressed SE genes observed here.

CDK8/19 depletion also modestly decreased the expression of many colon cancer SE genes. In contrast, inhibition of CDK8/19 kinase activity by cortistatin A identified CDK8/19 as SE gene repressors in mouse AML (23). Interestingly, in HCT116 cells, CDK8/19 inhibition by cortistatin A or depletion by use of shRNA causes distinct effects on transcription, suggesting kinase activity-independent functions for CDK8 and CDK19 (22), as recently reported for CDK19 in osteosarcoma cells (29). The positive role of CDK8/19 observed here might reflect the function of CDK8 as a stimulator of elongation via recruitment of pTEFb and BRD4 (19).

Although our results support transcriptional coregulation between the Mediator kinase module and BRD4 in colon cancer cells, MED12 or MED13/13L depletion had more specific effects than those of BRD4 depletion on cancer SE genes. BET inhibitors are currently being investigated as potent cancer drugs because of their specific effect on superenhancers in hematopoietic cancers (4–6). In the present study, SE genes were also significantly more decreased by BRD4 depletion than the rest of the expressed genome. Yet SE genes were not more sensitive to BRD4 depletion than control genes (non-SE and colon SE genes) that also had decreased expression following BRD4 depletion. Our results thus suggest that depletion of MED12/13/13L in colon cancer may provide a more specific targeting of cancer-acquired SE genes than BRD4 inhibition.

The strongest effects on SE gene expression and proliferation were seen with combined depletion of MED12 or MED13/13L together with BRD4, suggesting at least partly independent mechanisms of SE gene activation. In line with this, some Mediator-bound superenhancers appear to be unaffected by BRD4 inhibition by JQ1 in mouse AML cells (14). Interestingly, for triple-negative breast cancer (TNBC) cells, resistance to JQ1 was recently shown to involve BET-independent Mediator recruitment to acquired superenhancers (8). Thus, dual targeting of BRD4 and Mediator may provide a therapeutic opportunity more broadly in cancer treatment.

MATERIALS AND METHODS

Cell culture and RNA interference. Colon cancer HCT116 and DLD1 cells and human normal colon CCD841 CoN (ATCC CRL-1790) cells were cultured in McCoy's 5A medium (Gibco), RPMI medium (Lonza), and Eagle's minimum essential medium (EMEM) (Lonza), respectively, supplemented with 10% fetal bovine serum (FBS) (Gibco), L-glutamine, and antibiotics. Cells were seeded for experiments 1 day before transfection. Cells were transfected with Dharmacon siRNAs (20 pmol/target/ml of medium) (see Table S4 in the supplemental material) in antibiotic-free medium by use of Lipofectamine RNAi Max according to standard protocols, and the medium was changed 4 h later. siNT (nontargeting) was used to achieve the same final amount of siRNAs in single knockdowns as that in combination knockdowns. The

transfection was repeated the following day. Cells were analyzed 24, 48, or 72 h after the medium change of the initial siRNA transfection. Pools of 4 siRNAs were used in all experiments except the experiment presented in Fig. 1C, in which 2 individual siRNAs/target were used (Table S4).

Western blotting and quantitative PCR. Cells were lysed in boiling Laemmli buffer for Western blotting or in RNA lysis buffer (Qiagen RNeasy Plus or Macherey-Nagel NucleoSpin RNA Plus) for qPCR. Protein lysates were run in SDS-PAGE gels and blotted onto nitrocellulose membranes. After blocking of the membranes in 5% nonfat milk–Tris-buffered saline (TBS)–0.01% Tween, membranes were incubated with primary antibodies (listed in Table S5) overnight and detected using standard chemiluminescence protocols. Total RNA was extracted according to the protocols of the indicated manufacturers. cDNA synthesis was performed using Multiscribe reverse transcriptase (Life Technologies) and random hexamer primers. qPCR was performed using an Applied Biosystems Step-One Plus platform, Kapa Biosystems SYBR Fast reagents, and the oligonucleotides listed in Table S6.

RNA sequencing. HCT116 cells were transfected with siRNAs as described above. RNA was extracted using Qiagen RNeasy Plus standard methods with additional DNase treatment (Qiagen RNase-free DNase set). Total RNA (2.5 μg) was treated with Illumina Ribo-Zero rRNA removal reagent, and cDNA libraries were generated using an NEBNext Ultra Directional RNA library prep kit. Libraries were sequenced using an Illumina NextSeq 500 system. No significant differences in RNA amounts were observed between samples prior to and after rRNA removal (Table S7).

RNA-seq fastq files (1×; 75-bp reads) were trimmed for adaptor contamination by use of the Trimmomatic tool (30) before mapping to the reference human genome (GRCh38, release 24, from the Genecode website). Reads were aligned to the primary assembly genome by use of RNA-STAR (version 2.4) (31), and summarization of read counts at the gene level was assessed with the parameter "-quantMode GeneCounts" provided inside the RNA-STAR aligner. The matrix of raw counts was uploaded to the R/Bioconductor environment, and differential gene expression analysis was done using the limma/voom package (32). Only genes with more than 1 count per million (cpm) in at least 3 libraries were included in the analysis. Counts were transformed to $\log_2$ cpm and quantile normalized using the voom function from the limma/voom package. *P* values were adjusted to control for the global false-discovery rate (FDR) across comparisons, using the "global" option in decideTests. Genes were considered to be differentially expressed if the adjusted *P* value was smaller than 0.05. Gene set enrichment analysis and hypergeometric probability tests were performed using the GSEA platform (33, 34) and GeneProf (35), respectively. Other data sets used in this study were as follows: siCTNNB1 RNA-seq data (ArrayExpress accession number E-MTAB-651 [33]) ($\log_2$ fold change of $\geq$0.59; adjusted *P* value of $<$0.05), data from shBRD4 (GEO accession number GSE73317) and JQ1 (GEO accession number GSE73318) RNA-seq in HCT116 cells (16), H3K27ac chromatin immunoprecipitation sequencing (ChIP-seq) data (GEO accession number GSM945853) (1, 36), and a catalog of superenhancers (1). Superenhancer-associated genes (SE genes) (Table S2) specific or common to HCT116 cells or sigmoid colon samples (1) and with more than 1 cpm in at least 3 libraries from siNT RNA-seq were considered.

ChIP. HCT116 cells were transfected with siRNA as described above, and enhancer H3K27ac levels were assayed 72 h later using standard ChIP protocols. Briefly, chromatin was cross-linked in 1.1% paraformaldehyde (PFA) for 15 min at room temperature, and cells were lysed in standard ChIP lysis buffer containing 1% SDS. Sonication with a Misonics 4000 sonicator (PST Technics) was used to shear chromatin, and SDS-containing lysates were diluted five times for IP. Diluted lysates were incubated with 5 μg of antibody against H3K27ac (ab4729; Abcam) or MED12 (A300-774A; Bethyl Laboratories) overnight, and chromatin was pulled down by incubation with protein A-Sepharose beads blocked with herring sperm DNA. Following washing steps, chromatin was eluted in proteinase K solution and reverse cross-linked by incubation in 200 mM NaCl at 65°C overnight. Purified DNA was detected using qPCR as described above, and % input was calculated compared to the input samples taken before IP. Sequences of ChIP primers are listed in Table S6.

Proliferation assays. For cell counting, cells were washed twice with phosphate-buffered saline (PBS), detached by use of trypsin, and suspended to a single-cell suspension. Viable cells were counted using trypan blue staining. The amount of cells per milliliter of growth medium was compared to that for the indicated control sample. For EdU incorporation assays, cells were seeded on coverslips 1 day before the initial siRNA transfection. Transfections were performed as described above. Cells were exposed to 10 μM EdU in normal growth medium for 2 h prior to fixation in 4% PFA. EdU-positive cells were visualized by use of a Click-iT EdU Alexa Fluor 488 imaging kit, and nuclei were stained with Hoechst dye. The percentage of EdU-positive cells compared to total nuclei was quantified using Fiji software.

Dual-Luciferase assay. Caco-2 cells were maintained in RPMI medium (Lonza) supplemented with 20% FBS (Gibco), L-glutamine, and antibiotics. Cell were transfected with siRNA as described above. Two days before lysis, cells were transfected with TOPFlash-luciferase and TK-renilla plasmids by use of Fugene6 according to standard protocols. Cells were lysed in passive lysis buffer, a Dual-Luciferase assay (Promega) was performed, and luminescence was detected using a Fluostar Omega plate reader.

Accession number(s). RNA-seq data from this study can be accessed through Array Express under accession number E-MTAB-5873.

SUPPLEMENTAL MATERIAL

Supplemental material for this article may be found at https://doi.org/10.1128/MCB.00573-17.

SUPPLEMENTAL FILE 1, PDF file, 3.1 MB.

ACKNOWLEDGMENTS

This work was supported by grants from the Academy of Finland (projects 1259278 and 12718454), Biocentrum Helsinki, Finnish cancer organizations, and the Sigrid Juselius Foundation to T.P.M. and by grants from Svenska Kulturfonden, the K. Albin Johansson Foundation, the Oskar Öflund Foundation, the Biomedicum Helsinki Foundation, the Ida Montin Foundation, and the Paulo Foundation to E.K.

We thank the members of the Mäkelä laboratory for comments on the manuscript and Alisa Kopilow for technical assistance. E.K. is a student in the Doctoral Program of Biomedicine (DPBM). RNA sequencing was performed at the Biomedicum Functional Genomics Unit (FuGu). The CDK8 antibody was a kind gift from Erich Nigg.

We report that we have no conflicts of interest.

REFERENCES

1. Hnisz D, Abraham BJ, Lee TI, Lau A, Saint-Andre V, Sigova AA, Hoke HA, Young RA. 2013. Super-enhancers in the control of cell identity and disease. Cell 155:934–947. https://doi.org/10.1016/j.cell.2013.09.053.
2. Loven J, Hoke HA, Lin CY, Lau A, Orlando DA, Vakoc CR, Bradner JE, Lee TI, Young RA. 2013. Selective inhibition of tumor oncogenes by disruption of super-enhancers. Cell 153:320–334. https://doi.org/10.1016/j.cell.2013.03.036.
3. Whyte WA, Orlando DA, Hnisz D, Abraham BJ, Lin CY, Kagey MH, Rahl PB, Lee TI, Young RA. 2013. Master transcription factors and mediator establish super-enhancers at key cell identity genes. Cell 153:307–319. https://doi.org/10.1016/j.cell.2013.03.035.
4. Chapuy B, McKeown MR, Lin CY, Monti S, Roemer MG, Qi J, Rahl PB, Sun HH, Yeda KT, Doench JG, Reichert E, Kung AL, Rodig SJ, Young RA, Shipp MA, Bradner JE. 2013. Discovery and characterization of super-enhancer-associated dependencies in diffuse large B cell lymphoma. Cancer Cell 24:777–790. https://doi.org/10.1016/j.ccr.2013.11.003.
5. Roderick JE, Tesell J, Shultz LD, Brehm MA, Greiner DL, Harris MH, Silverman LB, Sallan SE, Gutierrez A, Look AT, Qi J, Bradner JE, Kelliher MA. 2014. c-Myc inhibition prevents leukemia initiation in mice and impairs the growth of relapsed and induction failure pediatric T-ALL cells. Blood 123:1040–1050. https://doi.org/10.1182/blood-2013-08-522698.
6. Roe JS, Mercan F, Rivera K, Pappin DJ, Vakoc CR. 2015. BET bromodomain inhibition suppresses the function of hematopoietic transcription factors in acute myeloid leukemia. Mol Cell 58:1028–1039. https://doi.org/10.1016/j.molcel.2015.04.011.
7. Korb E, Herre M, Zucker-Scharff I, Darnell RB, Allis CD. 2015. BET protein Brd4 activates transcription in neurons and BET inhibitor Jq1 blocks memory in mice. Nat Neurosci 18:1464–1473. https://doi.org/10.1038/nn.4095.
8. Shu S, Lin CY, He HH, Witwicki RM, Tabassum DP, Roberts JM, Janiszewska M, Huh SJ, Liang Y, Ryan J, Doherty E, Mohammed H, Guo H, Stover DG, Ekram MB, Peluffo G, Brown J, D'Santos C, Krop IE, Dillon D, McKeown M, Ott C, Qi J, Ni M, Rao PK, Duarte M, Wu SY, Chiang CM, Anders L, Young RA, Winer EP, Letai A, Barry WT, Carroll JS, Long HW, Brown M, Liu XS, Meyer CA, Bradner JE, Polyak K. 2016. Response and resistance to BET bromodomain inhibitors in triple-negative breast cancer. Nature 529:413–417. https://doi.org/10.1038/nature16508.
9. Allen BL, Taatjes DJ. 2015. The Mediator complex: a central integrator of transcription. Nat Rev Mol Cell Biol 16:155–166. https://doi.org/10.1038/nrm3951.
10. Kuuluvainen E, Hakala H, Havula E, Sahal Estime M, Ramet M, Hietakangas V, Makela TP. 2014. Cyclin-dependent kinase 8 module expression profiling reveals requirement of mediator subunits 12 and 13 for transcription of Serpent-dependent innate immunity genes in Drosophila. J Biol Chem 289:16252–16261. https://doi.org/10.1074/jbc.M113.541904.
11. Kim S, Xu X, Hecht A, Boyer TG. 2006. Mediator is a transducer of Wnt/beta-catenin signaling. J Biol Chem 281:14066–14075. https://doi.org/10.1074/jbc.M602696200.
12. Kagey MH, Newman JJ, Bilodeau S, Zhan Y, Orlando DA, van Berkum NL, Ebmeier CC, Goossens J, Rahl PB, Levine SS, Taatjes DJ, Dekker J, Young RA. 2010. Mediator and cohesin connect gene expression and chromatin architecture. Nature 467:430–435. https://doi.org/10.1038/nature09380.
13. Aranda-Orgilles B, Saldana-Meyer R, Wang E, Trompouki E, Fassl A, Lau S, Mullenders J, Rocha PP, Raviram R, Guillamot M, Sanchez-Diaz M, Wang K, Kayembe C, Zhang N, Amoasii L, Choudhuri A, Skok JA, Schober M, Reinberg D, Sicinski P, Schrewe H, Tsirigos A, Zon LI, Aifantis I. 2016. MED12 regulates HSC-specific enhancers independently of mediator kinase activity to control hematopoiesis. Cell Stem Cell 19:784–799. https://doi.org/10.1016/j.stem.2016.08.004.
14. Bhagwat AS, Roe JS, Mok BY, Hohmann AF, Shi J, Vakoc CR. 2016. BET bromodomain inhibition releases the Mediator complex from select cis-regulatory elements. Cell Rep 15:519–530. https://doi.org/10.1016/j.celrep.2016.03.054.
15. Sur IK, Hallikas O, Vaharautio A, Yan J, Turunen M, Enge M, Taipale M, Karhu A, Aaltonen LA, Taipale J. 2012. Mice lacking a Myc enhancer that includes human SNP rs6983267 are resistant to intestinal tumors. Science 338:1360–1363. https://doi.org/10.1126/science.1228606.
16. McCleland ML, Mesh K, Lorenzana E, Chopra VS, Segal E, Watanabe C, Haley B, Mayba O, Yaylaoglu M, Gnad F, Firestein R. 2016. CCAT1 is an enhancer-templated RNA that predicts BET sensitivity in colorectal cancer. J Clin Invest 126:639–652. https://doi.org/10.1172/JCI83265.
17. Firestein R, Bass AJ, Kim SY, Dunn IF, Silver SJ, Guney I, Freed E, Ligon AH, Vena N, Ogino S, Chheda MG, Tamayo P, Finn S, Shrestha Y, Boehm JS, Jain S, Bojarski E, Mermel C, Barretina J, Chan JA, Baselga J, Tabernero J, Root DE, Fuchs CS, Loda M, Shivdasani RA, Meyerson M, Hahn WC. 2008. CDK8 is a colorectal cancer oncogene that regulates beta-catenin activity. Nature 455:547–551. https://doi.org/10.1038/nature07179.
18. Donner AJ, Ebmeier CC, Taatjes DJ, Espinosa JM. 2010. CDK8 is a positive regulator of transcriptional elongation within the serum response network. Nat Struct Mol Biol 17:194–201. https://doi.org/10.1038/nsmb.1752.
19. Galbraith MD, Allen MA, Bensard CL, Wang X, Schwinn MK, Qin B, Long HW, Daniels DL, Hahn WC, Dowell RD, Espinosa JM. 2013. HIF1A employs CDK8-mediator to stimulate RNAPII elongation in response to hypoxia. Cell 153:1327–1339. https://doi.org/10.1016/j.cell.2013.04.048.
20. Tsai KL, Sato S, Tomomori-Sato C, Conaway RC, Conaway JW, Asturias FJ. 2013. A conserved Mediator-CDK8 kinase module association regulates Mediator-RNA polymerase II interaction. Nat Struct Mol Biol 20:611–619. https://doi.org/10.1038/nsmb.2549.
21. Turunen M, Spaeth JM, Keskitalo S, Park MJ, Kivioja T, Clark AD, Makinen N, Gao F, Palin K, Nurkkala H, Vaharautio A, Aavikko M, Kampjarvi K, Vahteristo P, Kim CA, Aaltonen LA, Varjosalo M, Taipale J, Boyer TG. 2014. Uterine leiomyoma-linked MED12 mutations disrupt mediator-associated CDK activity. Cell Rep 7:654–660. https://doi.org/10.1016/j.celrep.2014.03.047.
22. Poss ZC, Ebmeier CC, Odell AT, Tangpeerachaikul A, Lee T, Pelish HE, Shair MD, Dowell RD, Old WM, Taatjes DJ. 2016. Identification of Mediator kinase substrates in human cells using cortistatin A and quantitative phosphoproteomics. Cell Rep 15:436–450. https://doi.org/10.1016/j.celrep.2016.03.030.
23. Pelish HE, Liau BB, Nitulescu II, Tangpeerachaikul A, Poss ZC, Da Silva DH, Caruso BT, Arefolov A, Fadeyi O, Christie AL, Du K, Banka D, Schneider EV, Jestel A, Zou G, Si C, Ebmeier CC, Bronson RT, Krivtsov AV, Myers AG, Kohl NE, Kung AL, Armstrong SA, Lemieux ME, Taatjes DJ, Shair MD. 2015. Mediator kinase inhibition further activates super-enhancer-associated genes in AML. Nature 526:273–276. https://doi.org/10.1038/nature14904.
24. Hnisz D, Schuijers J, Lin CY, Weintraub AS, Abraham BJ, Lee TI, Bradner JE, Young RA. 2015. Convergence of developmental and oncogenic

signaling pathways at transcriptional super-enhancers. Mol Cell 58: 362–370. https://doi.org/10.1016/j.molcel.2015.02.014.
25. Moffa G, Erdmann G, Voloshanenko O, Hundsrucker C, Sadeh MJ, Boutros M, Spang R. 2016. Refining pathways: a model comparison approach. PLoS One 11:e0155999. https://doi.org/10.1371/journal.pone.0155999.
26. Sansom OJ, Meniel VS, Muncan V, Phesse TJ, Wilkins JA, Reed KR, Vass JK, Athineos D, Clevers H, Clarke AR. 2007. Myc deletion rescues Apc deficiency in the small intestine. Nature 446:676–679. https://doi.org/10.1038/nature05674.
27. McCleland ML, Soukup TM, Liu SD, Esensten JH, de Sousa e Melo F, Yaylaoglu M, Warming S, Roose-Girma M, Firestein R. 2015. Cdk8 deletion in the Apc(Min) murine tumour model represses EZH2 activity and accelerates tumourigenesis. J Pathol 237:508–519. https://doi.org/10.1002/path.4596.
28. Filippakopoulos P, Qi J, Picaud S, Shen Y, Smith WB, Fedorov O, Morse EM, Keates T, Hickman TT, Felletar I, Philpott M, Munro S, McKeown MR, Wang Y, Christie AL, West N, Cameron MJ, Schwartz B, Heightman TD, La Thangue N, French CA, Wiest O, Kung AL, Knapp S, Bradner JE. 2010. Selective inhibition of BET bromodomains. Nature 468:1067–1073. https://doi.org/10.1038/nature09504.
29. Audetat KA, Galbraith MD, Odell AT, Lee T, Pandey A, Espinosa JM, Dowell RD, Taatjes DJ. 2017. A kinase-independent role for cyclin-dependent kinase 19 in p53 response. Mol Cell Biol 37:e00626-16. https://doi.org/10.1128/MCB.00626-16.
30. Bolger AM, Lohse M, Usadel B. 2014. Trimmomatic: a flexible trimmer for Illumina sequence data. Bioinformatics 30:2114–2120. https://doi.org/10.1093/bioinformatics/btu170.
31. Dobin A, Davis CA, Schlesinger F, Drenkow J, Zaleski C, Jha S, Batut P, Chaisson M, Gingeras TR. 2013. STAR: ultrafast universal RNA-seq aligner. Bioinformatics 29:15–21. https://doi.org/10.1093/bioinformatics/bts635.
32. Ritchie ME, Phipson B, Wu D, Hu Y, Law CW, Shi W, Smyth GK. 2015. limma powers differential expression analyses for RNA-sequencing and microarray studies. Nucleic Acids Res 43:e47. https://doi.org/10.1093/nar/gkv007.
33. Mootha VK, Lindgren CM, Eriksson KF, Subramanian A, Sihag S, Lehar J, Puigserver P, Carlsson E, Ridderstrale M, Laurila E, Houstis N, Daly MJ, Patterson N, Mesirov JP, Golub TR, Tamayo P, Spiegelman B, Lander ES, Hirschhorn JN, Altshuler D, Groop LC. 2003. PGC-1alpha-responsive genes involved in oxidative phosphorylation are coordinately downregulated in human diabetes. Nat Genet 34:267–273. https://doi.org/10.1038/ng1180.
34. Subramanian A, Tamayo P, Mootha VK, Mukherjee S, Ebert BL, Gillette MA, Paulovich A, Pomeroy SL, Golub TR, Lander ES, Mesirov JP. 2005. Gene set enrichment analysis: a knowledge-based approach for interpreting genome-wide expression profiles. Proc Natl Acad Sci U S A 102:15545–15550. https://doi.org/10.1073/pnas.0506580102.
35. Halbritter F, Vaidya HJ, Tomlinson SR. 2011. GeneProf: analysis of high-throughput sequencing experiments. Nat Methods 9:7–8. https://doi.org/10.1038/nmeth.1809.
36. ENCODE Project Consortium. 2012. An integrated encyclopedia of DNA elements in the human genome. Nature 489:57–74. https://doi.org/10.1038/nature11247.